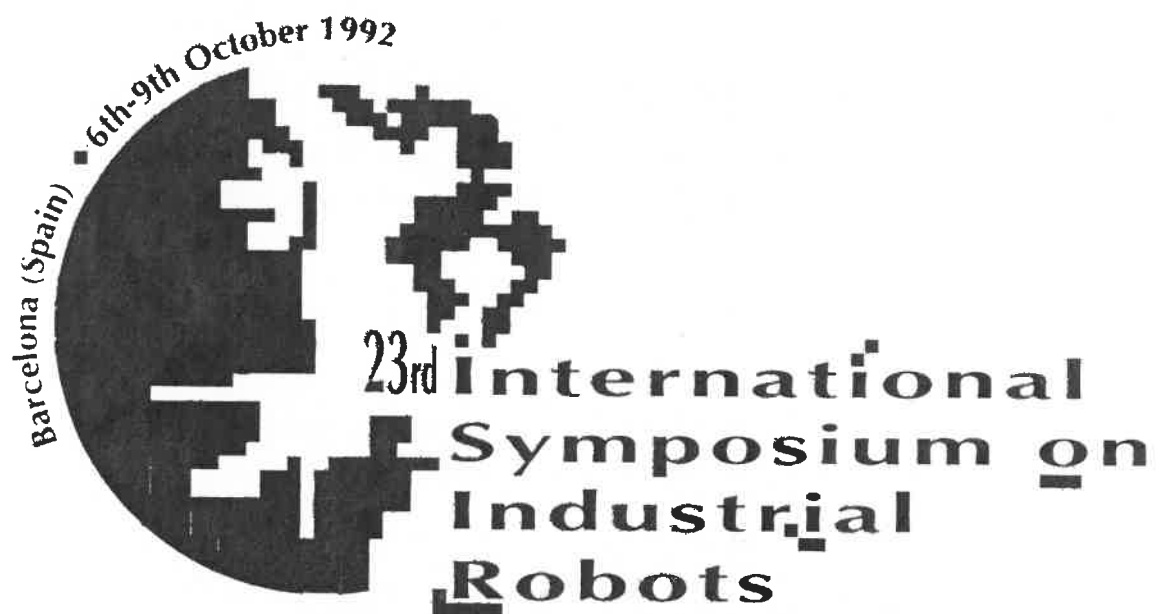


# PROCEEDINGS



# ILLUSTRATING AN AUTOMATIC PLANNER FOR ROBOTIC ASSEMBLY TASK\*

Luis Basañez and Raúl Suárez  
Institut de Cibernètica (UPC-CSIC)  
Diagonal 647, 08028 Barcelona, Spain

## ABSTRACT

The paper shows the working of a previously proposed automatic fine-motion planner for assembly tasks with robots by means of a simple but illustrative case: the block in the corner problem. The assembly planner takes into consideration the different uncertainty sources that can affect the task and the friction forces produced by the relative movements of the objects in contact. The results of the planning procedure steps applied to the above mentioned case are mainly shown in a graphical way giving at the same time its physical interpretation. This allows to get a better inside onto the proposed methodology and its possibilities.

**Keywords.** Robots; Assembly; Uncertainty; Planning.

## 1. INTRODUCTION

Assembly is one of the most promising fields of application of industrial robots in a near future. Nevertheless, assembly with robots still exhibits some basic problems especially when uncertainty in robot positioning is comparable to parts mating clearance.

In order to efficiently perform assembly tasks with robots, several solutions, like robot precision increasing and passive compliance devices, have been proposed. A further simplification of these tasks could be achieved by a better design of the parts and objects involved in them.

Despite these improvements, performing assembly tasks in a more flexible way requires the use of *active compliance* – based on position/force control – whose main advantage is the possibility of adapting the compliance parameters during the development of the task.

The assembly strategies associated to the use of active compliance could be generated by a human operator, but they are task-dependent and frequently they imply great skill and effort. Consequently, it becomes evident the interest of an automatic fine motion planner capable of establish a sequence of movements that assure assembly task success despite uncertainty.

The use of position/force control to compensate uncertainty in assembly tasks was introduced by Inoue (1974) and, from that, several approaches to automatic generation of assembly strategies based on position/force control have been developed (Dufay and Latombe, 1984; Turk, 1985; Lozano Perez, Mason and Taylor, 1984; Erdmann, 1984; Buckley, 1987; Xiao and Volz, 1989; Gottschlich and Kak, 1991).

In previous papers (Suárez and Basañez, 1989, 1991), we have proposed a fine motion planner for assembly tasks which takes into consideration a great variety of uncertainties and friction forces. This planner has been completely developed for rigid

polyhedral objects and planar movements (i.e. two translational and one rotational degrees of freedom). Tasks with more degrees of freedom could be theoretically solved by a planner based on the same principles, but additional research work would be required in order to maintain the efficiency.

In this paper we illustrate the functioning of the proposed assembly task planner through a simple example. Section 2 of the paper briefly explains the planner. Firstly, the different steps of the plan generation are outlined. Then, the uncertainty sources are described and, finally, task modelling, planning and execution are commented. Section 3 is dedicated to the development of the selected planning example: *the block in the corner problem*. Finally, in section 4 the main conclusions are outlined.

## 2. THE ASSEMBLY PLANNER

### 2.1. Overview

The goal of the assembly planner is to generate a sequence of commands to be successively applied to the robot controller in order to successfully perform the assembly task. These robot commands depend on the type of robot controller used. Assuming a robot controller able to work in damping control mode (Whitney, 1977) robot commands will be commanded velocities.

In the following we assume that the objects are polyhedral, that is, its nominal faces are flat although small curvature in the faces due to their manufacturing tolerances are acceptable. The objects can also be considered rigid under the forces developed in its manipulation.

Additionally it is assumed that the edges of the object in the robot gripper or the edges of every static object in the work space or all the edges simultaneously are parallel or perpendicular to the plane of movement. In this way, 3D objects moved in a plane can be modelled as 2D objects moved in a plane parallel to it.

The input data to the planner are, in addition to the task goal, the shape and size of all the objects involved in the task, their

\*This work was partially supported by *Comisión Interministerial de Ciencia y Tecnología (CICYT)* under the project ROB 89-0287

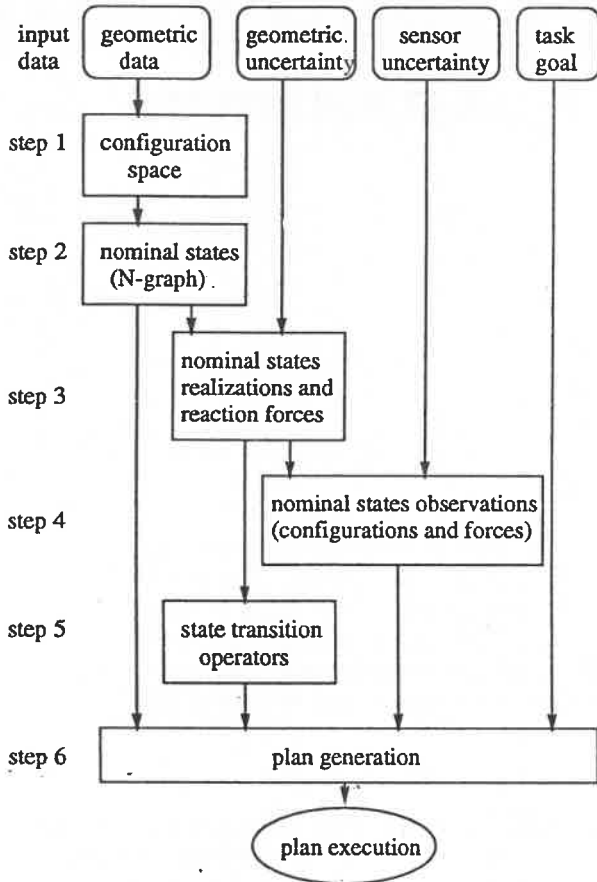


Fig. 1. Planning scheme.

manufacturing tolerances, the position accuracy of the robot and the accuracy of the different sensors used to locate the objects and to measure the forces and torques.

The main planning steps are shown in Fig. 1. The first step is the construction of the *Configuration Space*, ( $C$ ) (Lozano Perez, 1983). In order to describe the configuration of an object being moved on a plane by a robot, we choose a reference point  $P_r$  fixed to the gripper (e.g. the TCP point) represented by  $\vec{p}_r$  in the absolute reference system. The three degrees of freedom (two of translation and one of rotation) will be indicated by  $p_{rx}$ ,  $p_{ry}$  and  $\phi_r$  and thus a point of  $C$  will be represented by  $[p_{rx} \ p_{ry} \ \phi_r]^T$ .

Second step consist in the determination of the *nominal task states* according to the single or multiple basic contacts which could happen during task execution if uncertainty does not exist. Then, nominal states that could be consecutive during a nominal task execution are represented as a graph, *N-Graph*.

In the third step, geometric uncertainty other than related to on-line measurement is included, giving rise to state realizations in presence of uncertainty. From them, the sets of possible reaction force directions including friction are obtained for each state. In a similar way to  $C$ , force and torque components are represented using a unique vector  $\vec{g}$  called *generalized force*. The space that these vectors define is called *Generalized Force Space*,  $\mathcal{F}$ .

Next step correspond to the incorporation of the uncertainty due to the on-line measurement. The result is the *observation domain*, that is, the set of configurations and generalized reaction forces that could be measured when a given state occurs.

In the fifth step, a map of transition directions – *state transition operators* – is obtained for each state, labeling each movement

direction (i.e. commanded velocity direction) with the contiguous states that may be reached following it.

The generation of the assembly plan is the objective of the sixth and last step. This implies the search of a path in the *N-Graph* from the initial state to the goal one and the choice of the associated transition operators.

Plan execution consists basically in the identification of the current task state by fusing configuration and force/torque sensors information and, then, the application of the corresponding operator until a new state was detected

## 2.2. Uncertainty

Parameters and variables describing objects or objects' behavior in real world are not exactly known. In some robot tasks, like fine-motion planning, it is not enough to deal with *nominal* or *predicted* values, but some specification about their imprecision is necessary.

We will call *uncertainty* of a parameter or variable to the domain containing all possible actual values for an observed one subject to deviations. Uncertainties are represented by  $U$  with a subscript indicative of the related variable or parameter. Parameters used to describe maximum deviations are represented by  $\epsilon$  with the same subscript. The subscript  $o$  indicates an *observed* value, sensed or calculated.

In the following, we enumerate and model the sources of position, force and velocity uncertainty to be considered in a motion planning problem (Basañez and Suárez, 1991).

*Uncertainty of the shape and size of objects.* Describing the object boundary by using vectors  $\vec{v}$  referred to an object reference point  $P_g$ , object shape and size uncertainty is expressed through the vertex position uncertainty:

$$U_v = \{ \vec{v} \mid \| \vec{v} - \vec{v}_o \| \leq \epsilon_v \}$$

*Uncertainty of the position measurement of a point of a static object.* It entirely depends on the sensors or measurement system used to locate the point  $\vec{a}$ , but a generic model can be established as

$$U_m = \{ \vec{a} \mid \| \vec{a} - \vec{a}_o \| \leq \epsilon_m \}$$

*Uncertainty of the configuration of a static object.* The static object could be previously positioned by a feeder, for instance; but, in order to make the uncertainty model independent of any specific feeder, we assume that each object vertex is located inside a circle of radius  $\epsilon_{p_r}$  centered at the vertex predicted position.

*Uncertainty of the robot positioning.* Using  $\vec{p}_r$  and  $\phi_r$  to represent the real position and orientation of the end effector, the corresponding uncertainty will be modelled as,

$$U_{p_r} = \{ \vec{p}_r \mid \| \vec{p}_r - \vec{p}_{r0} \| \leq \epsilon_{p_r} \}$$

$$U_{\phi_r} = \{ \phi_r \mid | \phi_r - \phi_{r0} | \leq \epsilon_{\phi_r} \}$$

*Slide of the object in the gripper.* We model the slide of the object in the gripper assuming upper limits for translation,  $\epsilon_{p_d}$  and for rotation around the gripper reference point,  $\epsilon_{\phi_d}$ .

*Uncertainty of the reaction forces and torque measurements.* We will consider a wrist force/torque sensor that gives reaction forces as two orthogonal components and the torque about the gripper point given by  $\vec{p}_r$ . Uncertainty is a function of the

sensor accuracy and can be modeled as,

$$\begin{aligned} U_{f_x} &= \{f_x \mid \|f_x - f_{x0}\| \leq \epsilon_{f_x}\} \\ U_{f_y} &= \{f_y \mid \|f_y - f_{y0}\| \leq \epsilon_{f_y}\} \\ U_{\tau} &= \{\tau \mid \|\tau - \tau_0\| \leq \epsilon_{\tau}\} \end{aligned}$$

*Uncertainty of the mobile object velocity.* This uncertainty is due to the robot control system errors. Real velocity is bounded to be inside a cone whose axis direction is determined by the nominal velocity direction.

**Uncertainty of the Absolute Position of any Object Point.** With the proposed models the real position of any point of a static object is bounded to be inside a circle of radius  $\epsilon_a = \epsilon_v + \epsilon_{p_r}$  centered in the nominal point position. In the case of a grasped object, the absolute nominal position of a point is described by a vector from the gripper reference point; the bounds of the uncertainty are  $\epsilon_{p_r p_{gv}} = \epsilon_{p_r} + \epsilon_{p_g} + \epsilon_v$  with  $\epsilon_{p_g} = \epsilon_{p_r} + \epsilon_{p_p} + \epsilon_{p_d}$  for the head of this vector, and  $\epsilon_{\phi_r \phi_g} = \epsilon_{\phi_r} + \epsilon_{\phi_g}$  with  $\epsilon_{\phi_g} = \epsilon_{\phi_r} + \epsilon_{\phi_d}$  for its angle.

**Uncertainty in the Configuration Space.** Making use of the geometric uncertainties above mentioned it is possible to build the  $C$  with uncertainty and then to determine all the configurations in which a set of basic contacts would be possible (Basañez and Suárez, 1991). The set of configurations in which a given basic contact could happen in presence of uncertainty determines an *uncertainty region CU*; the union of  $CU$ 's of every basic contact contains all possible contact configurations in presence of uncertainty.

**Uncertainty in Generalized Force Space.** Uncertainty of generalized forces is due to deviations in the forces and torques measurements, and it must be distinguished from the change in the possible generalized reaction forces due to uncertainty in  $C$ . The geometric interpretation of generalize force uncertainty is a prism whose size is given by  $\epsilon_{f_x}$ ,  $\epsilon_{f_y}$  and  $\epsilon_{f_z}$ .

### 2.3. Task Modelling

During an assembly task execution, it is important to know which basic contacts take place in order to decide next movement. So, we define the task states according to basic contacts occurrence.

A set of edge-vertex basic contacts is said to be *compatible* if all the contacts can occur simultaneously. Then, for each compatible set  $\mathcal{E}$  of basic contacts between the mobile object and the environment, a *task state E* is defined as the set of connected configurations in which all basic contacts of  $\mathcal{E}$ , and only those, occur.

States determined from a nominal task model, i.e. without uncertainty, are called *nominal task states*. They have a clear geometric interpretation: each  $C$ -face (without the  $C$ -edges), each  $C$ -edge (without the  $C$ -vertices) and each  $C$ -vertex of contact configurations of  $C$  conforms a different nominal state.

Nominal states are represented as nodes of a graph, *N-Graph*, which edges link those states that could be consecutive during a nominal task execution.

Directions of *generalized reaction forces* expected in a nominal state with only one basic contact are those in the generalized friction cones computed for the corresponding  $C$ -face. For nominal states with more than one basic contact the possible directions of reaction forces are obtained by a lineal combination of vectors from the generalized friction cone of each contact. For the planar problem, generalized forces directions are graphically represented by the method described by Brost and Mason (1989).

We define *state realization, R*, as the set of configurations in which that state can occur due to uncertainty. States realization and the corresponding generalized reaction forces can be obtained from the corresponding  $CU$  uncertainty regions built for  $\epsilon_{p_r} = 0$  and  $\epsilon_{\phi_r} = 0$ .

During task execution the actual state must be observed and recognized in order to apply a proper robot command. A state may be identified by using configuration and/or force measurements.

The *set of possible sensed configurations S* for task states with only one basic contact are fully equivalent to  $CU$  uncertainty regions of the corresponding  $C$ -face including all the uncertainties. Sets  $S$  of states with more than one basic contact are obtained by intersecting  $CU$  regions of  $C$ -faces of each basic contact.

The *set of possible observed generalized reaction forces G* that could be sensed during each state occurrence are obtained by adding generalized force uncertainty to the sets of possible generalized reaction forces in the states realization.

Once the current state has been identified, during task execution, a proper robot command must be applied to change current state towards the goal one. This implies that each state must have associated *state transition operators* that produce transition to another predicted state. Due to uncertainty, transition to an unique predicted state is unlikely, but a set of possible reachable states can be established.

The set of operators between any two contiguous states,  $E_i$  and  $E_j$ , are obtained by computing all movement directions with positive component in the direction normal to the frontier between  $R_i$  and  $R_j$ ; even when  $R_i \cap R_j \neq \emptyset$ , the normal direction is chosen pointing into  $R_j$  from configurations of  $R_i$  outside  $R_j$ . The obtained set of direction is then enlarged by including velocity uncertainty. Thus, for each state, a map of transition directions can be obtained, labeling each movement direction (i.e. commanded velocity direction) with the contiguous states that may be reached following it.

### 2.4. Task Planning

With the elements previously introduced and developed, the planning procedure can be divided into the following steps:

1. *Choice* in  $N$ -Graph a *directed path* from the initial state to the goal state.
2. *Associate* to each state in the path a *set of operators* which allow transition to the consecutive state.
3. *Expand the path* with all the states reachable by the application of the operators associate to path's states. It will leave to a directed graph, called *E-graph*.
4. *Repeat steps 1, 2 and 3* but considering as initial states those terminal states in  $E$ -graph different from the goal.

In the final  $E$ -graph, two types of circuits can appear: *soft circuits* in which the associated operators do not have directions with opposite components, and *hard circuits* when this condition is not satisfied. If possible, hard circuits must be avoided in the plan.

### 2.5. Task Execution

Plan execution consists basically in the identification of the current task state by fusing configuration and force/torque sensors information and then apply the corresponding operator  $T$  until a new state was detected.

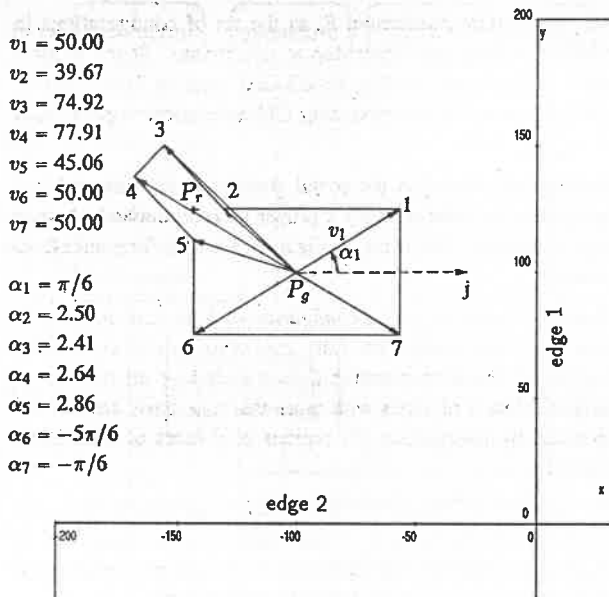


Fig. 2. Objects involved in the block-corner test problem

During plan execution, soft circuits if they appear, will be automatically broken. Hard circuits may really give rise to vicious circles during plan execution and therefore they must be specially monitored during on-line work. If they actually appear, an alternative plan must be executed starting from any state of the circuit.

### 3. THE BLOCK-IN-THE-CORNER PROBLEM

#### 3.1. Task Description and Assumptions

We will illustrate the proposed planning methodology by applying it to an example. It consists in a simple task that allows to show the development, step by step, of the planning procedure while maintaining the physical meaning of the problem. Despite it, the task gives enough possibilities to show how the planner works.

The selected task is the positioning of a block in a corner considering three degrees of freedom, two of translation and one of rotation. We will refer to this task as the *block-corner test problem*. One advantage of this problem is the easy 3D visualization of the associated  $C$ -surfaces.

In a planar representation, the block manipulated by the robot is basically a rectangular object with a handle. The corner, as part of a static object, is defined by two orthogonal edges. Both static and grasped objects are considered rigid. They are shown in Fig. 2 where, as in the rest of the paper, dimensions are indicated in millimeters, and angles in radians. The reference point of the block and of the gripper are  $P_g$  and  $P_r$ , respectively.

It is realistic to assume that the position reached by gross-motion movements is closed enough to the corner to assure contact with its edges during the first fine-motion movement; so, it will be taken as initial position for the assembly plan. It will also be assumed that the rotation of the block will never exceed  $\pm\pi/2$  from the final correct value.

We suppose a constant friction coefficient  $\mu = 0.7$ , to which it corresponds a friction cone of  $2 \times 0.61$ .

#### 3.2. Real World Uncertainty

Following the models previously described for the uncertainty

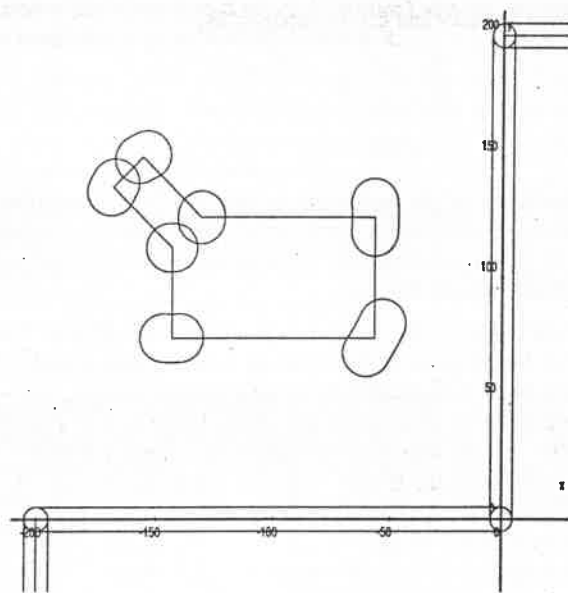


Fig. 3. Uncertainty in the absolute position of each block vertex and each corner edge.

sources, the maximum deviation values adopted are:

$$\begin{aligned} \epsilon_v &= 3 & \epsilon_{p_r} &= 1 & \epsilon_{p_d} &= 0 \\ \epsilon_m &= 5 & \epsilon_{\phi_r} &= \pi/90 & \epsilon_{\phi_d} &= 0 \\ \epsilon_{p_p} &= 5 & & & & \end{aligned}$$

then, the maximum deviation in the absolute position of any point of the static object will be:

$$\epsilon_a = 5$$

and the corresponding values for a point of the block will be:

$$\epsilon_{p_r p_g v} = 9 \quad \epsilon_{\phi_r \phi_g} = \pi/45$$

Figure 3 shows the boundaries of the sets of possible absolute positions of each block vertex—for the robot configuration  $[p_{rx} \ p_{ry} \ \phi_r]^T = [-143.3 \ 125 \ -\pi/4]^T$ —and of each corner edge.

Uncertainty in the force and torque measurements are modelled from the specifications of a commercial industrial wrist force-torque sensor, resulting

$$\epsilon_{f_x} = 0.1 \text{ N} \quad \epsilon_{f_y} = 0.1 \text{ N} \quad \epsilon_\tau = 0.001 \text{ Nm}$$

Robot velocity is bounded to be inside a cone with its axis in the nominal velocity direction and defined by an angle of  $\pi/30$ .

#### 3.3. Uncertainty in the Configuration and Force Spaces

Figure 4 shows  $C$  for the block-corner test problem in absence of uncertainty, built considering  $P_r$  as reference point. In the figure,  $C$ -surfaces are labeled with the corresponding contact  $c_{ij}$ , where  $i$  indicates the corner edge and  $j$  the block vertex involved in the contact.

Mapping the uncertainty into  $C$  is done following the equations developed by Basañez and Suárez (1991). As an example, Fig. 5 shows the uncertainty region  $CU$  of  $c_{11}$ . The boundary of this set of configurations is composed of ten different algebraic surfaces.

The set of all possible generalized reaction forces for  $c_{11}$  in presence of geometric uncertainty (including friction forces) is

shown in Fig. 6. In the general case, the boundary of these sets of generalized force directions are composed by sections of two hyperboles, six straight lines and a circumference.

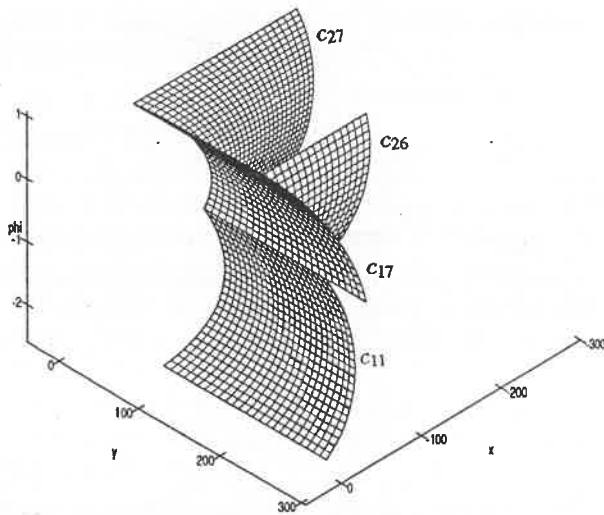


Fig. 4.  $C$  for the block-corner test problem.

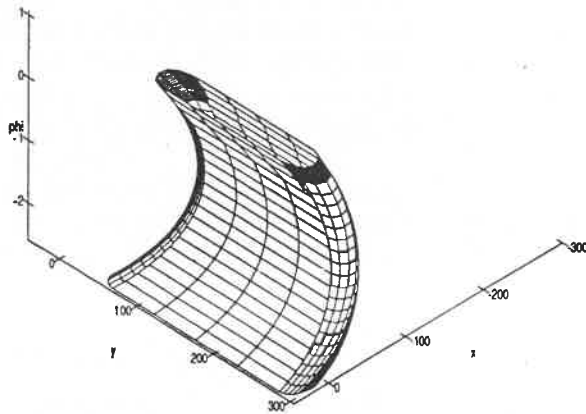


Fig. 5. Uncertainty  $CU$  corresponding to the contact  $c_{11}$ .

### 3.4. Task States

The block-corner test problem gives rise to nine nominal task states. We will represent them by  $E$  with a subscript composed by the couples of numbers used to describe the corresponding basic contacts.

Four states correspond to the four different possible basic contacts ( $C$ -surfaces in Fig. 4), i.e.  $E_{11}$ ,  $E_{17}$ ,  $E_{26}$  and  $E_{27}$ ; another four, to the possible occurrence of two basic contacts simultaneously ( $C$ -edges in Fig. 4, i.e.  $E_{11,17}$ ,  $E_{11,27}$ ,  $E_{26,27}$  and  $E_{26,17}$ ; and the last one corresponding to the occurrence of the four possible basic contact simultaneously ( $C$ -vertex in Fig. 4), i.e.  $E_{11,17,26,27}$ .

The N-Graph of nominal states is represented in Figure 7. It is easy to verify in the physical space the contiguity of any two states linked by an edge in the N-Graph. The goal state

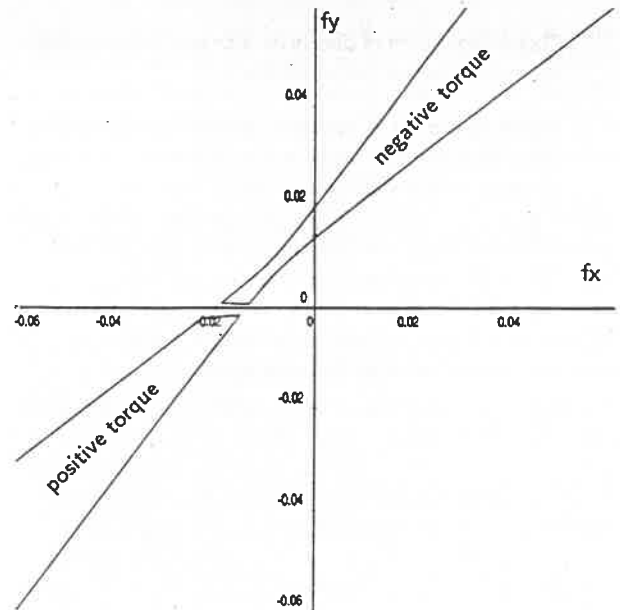


Fig. 6. Possible generalized reaction forces of contact  $c_{11}$  in presence of geometric uncertainty.

two states linked by an edge in the N-Graph. The goal state is obviously  $E_{11,17,26,27}$  and as initial state it will be considered  $E_{11}$ .

Taking into account all the uncertainty sources, the set of possible sensed configurations ( $S$ ) of each state is built. Since the set  $S$  of states with only one basic contact is equivalent to the corresponding uncertainty  $CU$ , Fig. 5 also represents the set  $S$  of the basic contact  $c_{11}$ . The set  $S$  of a state associated with several basic contacts is generated by intersecting the corresponding uncertainties  $CU$ ; for instance, Fig. 8 shows the set  $S$  of the state  $E_{11,27}$ .

The sets of all possible sensed generalized reaction forces ( $G$ ) for each state are also determined considering uncertainty. For states with an unique basic contact  $G$  is directly obtained by adding force measurement uncertainty to the forces that could happen in each state realization due to friction and geometric uncertainty (without considering robot configuration uncertainty because the sensor is fixed to the robot wrist). As an example, Fig. 6 shows  $G$  for  $c_{11}$ .

The sets of all possible sensed generalized reaction forces ( $G$ ) for states with an unique basic contact is directly obtained by adding force measurement uncertainty to the forces (showed in Fig. 6 for  $c_{11}$ ) that could happen in each state realization due to friction and geometric uncertainty (without considering robot configuration uncertainty because the sensor is fixed to the robot wrist).

For states with  $n$  basic contacts,  $G$  is obtained as the zone covered by all the lineal combinations of  $n$  forces, taking each of them from the set associated to each involved contact. Figure 9 shows the set of all possible generalized reaction forces for  $E_{11,27}$  in presence of geometric uncertainty and including friction forces.

### 3.5. Operators

Operators are equivalent to velocity commands to the robot control system. Transition operators between two states are determined in 4 steps:

1. Computing the set of directions orthogonal to the frontier between the realization domains of both states

2. Computing the set of directions with positive component in any direction of the set of step 1
3. Removing the set of opposite directions to the possible generalized reaction forces of the leaven state (to avoid jamming in that state)
4. Adding velocity uncertainty to directions resting after step 3

The operator  $T$  trying to perform transition between the two states must be chosen from the resulting set.

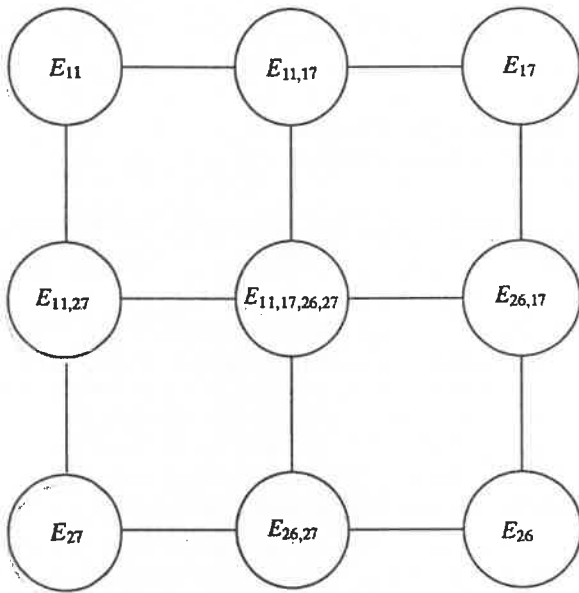


Fig. 7. Graph of nominal states.

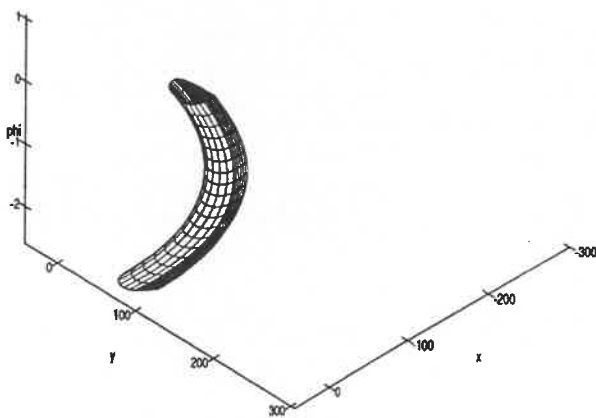


Fig. 8. Set of possible sensed configurations  $S$  for the state generated by the basic contacts  $c_{11}$  and  $c_{27}$ .

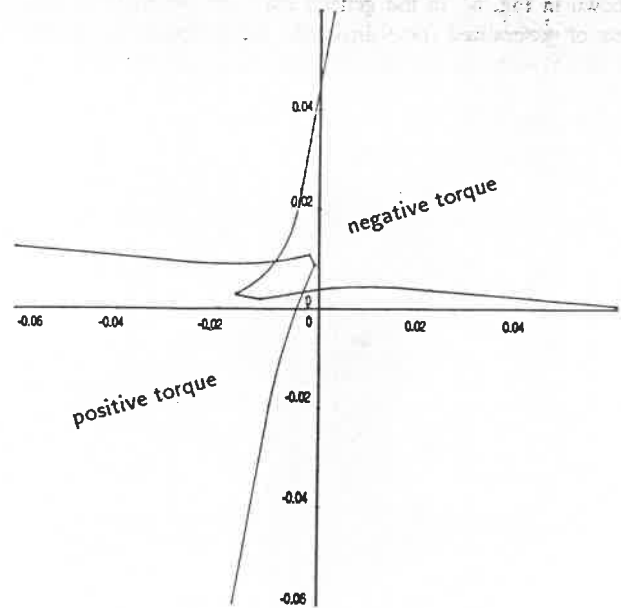


Fig. 9. Possible generalized reaction forces for  $E_{11,27}$  in presence of geometric uncertainty.

### 3.6. Planning and the Resulting Plan

The selected path of the N-Graph going from the initial to the goal states is:

$$E_{11} \rightarrow E_{11,17} \rightarrow E_{11,17,26,27}$$

The following operators  $T = [V_{rx} \ V_{ry} \ \Omega_r]^T$ , between the path states has been choiced:

$$\begin{aligned} \text{From } E_{11} \text{ to } E_{11,17} : & \quad [0 \ 0 \ 1]^T \\ \text{From } E_{11,17} \text{ to } E_{11,17,26,27} : & \quad [0 \ -1 \ 0]^T \end{aligned}$$

The operators producing transitions between the path states could give rise to transitions to other states. By including these states the path is expanded, resulting the final E-Graph showed in Fig. 10.

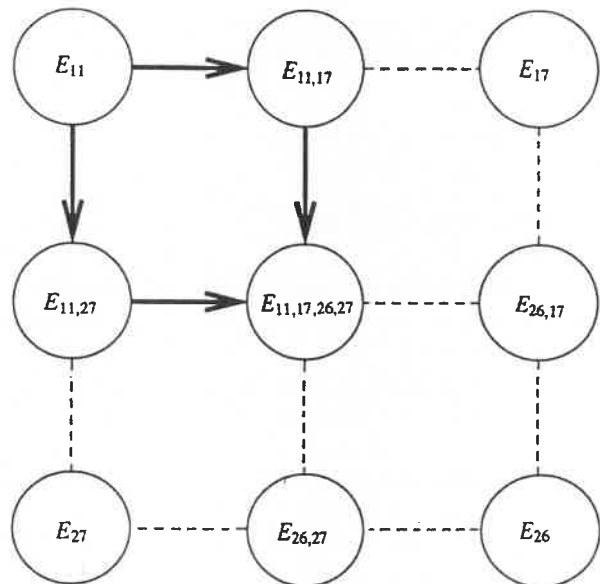


Fig. 10. Final E-Graph.

It is easy to visualize in the physical world, that most of the operators that would allow the transition from  $E_{11}$  to  $E_{11,17}$  also could permit transition to  $E_{11,27}$  if the block, maintaining contact  $c_{11}$ , is closed enough to edge 2 of the corner.

The resulting assembly plan for the block-corner test problem consists in the E-Graph showed in Fig. 10 plus the corresponding associated state transition operators.

#### 4. CONCLUSIONS

The block in the coner problem has allowed to show, in a graphical way and with references to the physical meaning, the working of an automatic fine-motion planner for assembly tasks with robots, that was previously proposed.

The planning methodology has been completely developed for two translational and one rotational degrees of freedom, and both the computing time and the memory requirements are fully acceptable for today workstations.

Nevertheless, several aspects of the planner, mainly related to the best selection of the state transition operator to be actually applied, are under research.

Another interesting subject for future research is error recovery during plan execution. Finally, as a more long term research, the extension of the planner to more than three degrees of freedom would be tried.

#### REFERENCES

- Basañez L. and R. Suárez (1991). Uncertainty Modelling in Configuration Space for Robotic Motion Planning. *Proc. of SYROCO'91*, Vienna, Austria, 675-680.
- Brost R. C. and M. Mason (1989). Graphical Analysis of Planar Rigid-Body Dynamics with Multiple Frictional Contacts. *Fifth Int. Symposium of Robotics Research*.
- Buckley, S.J. (1987). Planning and teaching compliant motion strategies. *MIT Art. Intell. Lab. report AI-TR-936 (Ph.D Thesis)*.

- Dufay, B., and J. Latombe (1984). An approach to automatic robot programming based on inductive learning. *Robotics Research: The First Int. Symposium*. The MIT Press., pp. 97-115.
- Erdmann, M. (1984). On motion planning with uncertainty. *MIT Art. Intell. Lab. report AI-TR-810*
- Gottschlich S. and A. Kak (1991). Motion Planning for Assembly Mating Operations *Proc. of the 1991 IEEE Int. Conference on Robotics and Automation*, California, USA, 1956-1963.
- Inoue H. (1974). Force Feedback in Precise Assembly Task. *MIT Art. Intell. Lab. Memo 308*.
- Lozano Perez, T. (1983). Spatial planning: a configuration space approach. *IEEE Trans. on Computers*, C-32 (2), 108-120.
- Lozano Perez, T., M. Mason, and R. Taylor (1984). Automatic synthesis of fine-motion strategies for robots. *The Int. Journal of Robotics Research*, 3 (1), 3-24.
- Suárez R. and L. Basañez (1989). Automatic Fine-Motion Planning based on Position/Force States. *Preprints of IFAC Symposium INCOM'89*, Madrid, Spain, 369-375.
- Suárez R. and L. Basañez (1991). Assembly with Robots in Presence of Uncertainty. *Proc. of the 22nd. ISIR*, Detroit, USA, 19.1-19.15.
- Turk, M.A. (1985). A fine-motion planning algorithm. *Intelligent Robots and Computer Vision - SPIE*, 579.
- Whitney, D. (1977). Force feedback control of manipulator fine motions. *Trans. of ASME Journal of Dyn. Syst., Meas., and Control*, June, 91-97.
- Xiao J. and R. Volz (1989). On replanning for Assembly Tasks Using Robots in the Presence of Uncertainties. *Proc. of the 1989 IEEE Int. Conf. on Robotics and Automation*, Arizona, USA, 638-645.